

RESEARCH ARTICLE

Geometric Analysis of Distributed Power Control and Möbius MAC Design

Zhen Tong^{1*} and Martin Haenggi¹¹Department of Electrical Engineering, University of Notre Dame, Notre Dame, IN, USA, 46556

ABSTRACT

This paper presents a geometric analysis of the convergence condition for the Foschini-Miljanic power control algorithm. The Möbius transform is exploited for the first time to analyze the convergence conditions of the power control algorithm. A novel MAC scheme based on the Möbius transform is proposed for the link scheduling problem and proven to improve spatial reuse by scheduling links in pairs if possible. The peak power constraint of wireless networks is analyzed theoretically, and applications to random networks are explored in detail. Observations from the analysis of peak power constraints are also applied to the design of the MAC scheme to improve the convergence speed and system performance. Applications to cognitive networks and heterogeneous networks are discussed. Copyright © 2010 John Wiley & Sons, Ltd.

KEYWORDS

Power Control; Möbius transform; Wireless Network

* Correspondence

Zhen Tong, Department of Electrical Engineering, University of Notre Dame, Notre Dame, IN, USA, 46556

Email: ztong1@nd.edu

1. INTRODUCTION

1.1. Motivation and Contribution

The Foschini-Miljanic (FM) power control algorithm in [1] is a distributed and dynamic power control algorithm to adjust transmit power levels using the instantaneous signal-to-interference Ratio (SIR) or signal-to-interference-and-noise Ratio (SINR) measured at the

receiver such that the SNR or SINR converges to a desired value. While the convergence condition of the FM power control algorithm has been well studied, it has not been analyzed from a geometric perspective. A geometric analysis can help researchers better understand the dependencies between the links in a wireless network and provide insight into the design of MAC schemes with dynamic power control. In this paper, we present such an analysis. An analytical tool that is novel in this context, the Möbius transform [2], is introduced to analyze the convergence condition. The analysis of the two-transmitter case illustrates that link nesting is possible with distributed and dynamic power control, which enables the design of MAC schemes that schedule link *pairs* instead of individual links.

A peak power constraint is an important factor that affects the convergence of dynamic power control algorithms. Existing dynamic power control algorithms with peak power constraint usually let the transmitters continue to transmit at peak power after the transmit power hits the power ceiling. However, their receivers' SINRs cannot achieve the desired SINR threshold. That is, while the convergence of the transmit powers is guaranteed, not all the receivers' SINRs converge to the desired threshold. Therefore, how to quantify the convergence of the receivers' SINRs under a peak power constraint is an unsolved problem. In this paper, a novel metric called *convergence probability* is defined to show the impact of the peak power constraint, and the properties and bounds of the convergence probability are derived theoretically for random networks.

Our main contributions are summarized as follows:

1. *Geometric analysis*: A novel analytical tool, the Möbius transform, is used for the geometric analysis of the convergence condition for the FM power control algorithm without fading.
2. *Peak power constraint*: The effects of the peak power constraints on the networks are studied in detail. Random networks are used for the first time to study the convergence of the dynamic power control algorithm with peak power constraint.
3. *Möbius MAC scheme*: A novel MAC scheme based on the geometric analysis and observations from peak power analysis is proposed to schedule link pairs with unequal link distances. Simulation results show that our MAC scheme is much more efficient to schedule links than the traditional CSMA scheme and has better quality of service (QoS) performance in terms of transport density.

1.2. Related Work

Transmission power control plays an important role in the design and operation of wireless networks. Much of the study on cellular network power control started in the 1990s and involved minimizing the total power while maintaining a fixed target SIR or SINR at the

desired receiver [1, 3, 4]. An efficient and distributed power control algorithm for cellular systems, now commonly referred to as the Foschini-Miljanic algorithm, was provided in [1]. The authors in [5] have shown the applicability of this algorithm to wireless ad hoc networks. Joint power control and scheduling algorithms have been proposed in [5, 6]. Different types of power control schemes for cellular systems have been presented in [7] and references therein. Recently, power control for various new types of wireless networks has been extensively studied, *e.g.*, [8] for two-tier femtocell networks and [9, 10] for cognitive radio networks. Moreover, constrained power control has been studied in [11, 12] since the maximum transmit power of a mobile user or any wireless transmitter is limited. The convergence of the distributed and dynamic power control algorithm with peak power constraint has been analyzed in [13, 14] for cellular networks.

A heuristic scheduling scheme is provided in [5] to determine a maximum subset of concurrently active links by shutting down the link with the minimum SINR until all the SINR requirements are satisfied. However, it is not distributed since one node needs all the SINR information from other nodes in order to decide if it can transmit or not. We propose a fully distributed MAC scheme that includes the peak power constraint in a natural way and schedules link in pairs. In our MAC scheme, called the Möbius MAC scheme, the geometric analysis that is derived from the two-transmitter case is utilized to serve as a criterion to schedule links in pairs.

1.3. Organization of the Paper

The rest of this paper is organized as follows. In Section II, the system model is introduced, assumptions stated and the metrics used in the paper defined. Section III discusses the convergence condition of the power control algorithm from a geometric perspective. The power control algorithm under the peak power constraint is also studied in detail in Section IV. Section V describes the novel energy-efficient MAC scheme. In Section VI, applications of our analysis to cognitive networks and heterogeneous networks are discussed. We conclude our work in Section VII.

2. SYSTEM MODEL

Consider a wireless network where all nodes share the same frequency band. Assume that the network has n links with each link consisting of a transmitter and its associated receiver. Thus, there are n transmitters and n receivers, and the sets of transmitting and receiving nodes are disjoint. An example of such a wireless network is illustrated in Fig. 1.

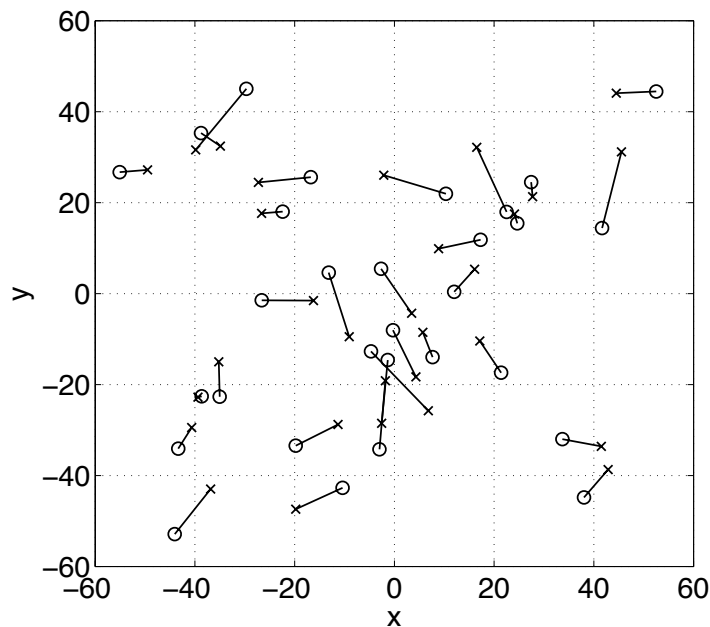


Figure 1. An example of the class of wireless networks considered in this paper. Crosses indicate the transmitters, and circles indicate the receivers.

The channel power gain from transmitter j to receiver i is denoted by h_{ij} . Note that fading is not considered throughout the paper. The QoS is represented by the SINR at the intended receiver. For a wireless network with n links, the SINR at the i th receiver is given by

$$\rho_i = \frac{h_{ii}P_i}{\sum_{j \neq i} h_{ij}P_j + \eta}, \quad (1)$$

where P_i is the power of the i th transmitter, and η is the noise power level.

3. CONVERGENCE CONDITION FOR POWER CONTROL

3.1. Review of Power Control Algorithm

Here we briefly review the power control algorithm proposed in [1]. The goal of the algorithm is to find the minimal solution of the transmit powers such that the SINR at each receiver meets a given threshold $\rho > 0$ required for acceptable performance. This constraint can be represented in matrix form as

$$(I - F)P \geq u, \quad (2)$$

where $P = (P_1, \dots, P_n)^T \in \mathbb{R}_+^n$ (denoted as $P > 0$) is the column vector of transmit powers,

$$u = \left(\frac{\rho\eta}{h_{11}}, \frac{\rho\eta}{h_{22}}, \dots, \frac{\rho\eta}{h_{nn}} \right)^T, \quad (3)$$

and F is a matrix with

$$F_{ij} = \begin{cases} 0, & \text{if } i = j \\ \frac{\rho h_{ij}}{h_{ii}}, & \text{if } i \neq j \end{cases} \quad (4)$$

where $i, j \in [n] \triangleq \{1, 2, \dots, n\}$.

The Perron–Frobenius eigenvalue σ_F of the matrix F is defined as the maximum modulus of all eigenvalues of F , i.e., $\sigma_F = \max_{1 \leq i \leq n} \{|\lambda_i|\}$, where $\lambda_1, \lambda_2, \dots, \lambda_n$ are the eigenvalues of F . From [1], if and only if $\sigma_F < 1$, $(I - F)^{-1}$ exists and $P^* = (I - F)^{-1}u > 0$ is the minimal power solution to (2). That is, if P is any other solution to (2), $P \geq P^*$ componentwise. Therefore, the total power consumption can be minimized by allocating the transmit powers P^* . $\sigma_F < 1$ also guarantees that the iterative distributed power control algorithm

$$P(k+1) = FP(k) + u, \quad (5)$$

or, equivalently,

$$P_i(k+1) = \frac{\rho}{\rho_i(k)} P_i(k) \quad (6)$$

converges to P^* , where $\rho_i(k)$ is the instantaneous SINR for i th receiver at time k , $P_i(k)$ is the power of the i th transmitter at time $k \in \mathbb{N}$, and the initial value $P(0)$ is given.

3.2. Geometric Analysis of the Convergence Condition in the Two-link Case

The path loss is assumed to be proportional to the γ th power of the distance between the transmitter and the receiver. The channel power gain from transmitter j to receiver i without fading is thus given by

$$h_{ij} = \left(\frac{d_0}{d_{ij}} \right)^\gamma, \quad (7)$$

where γ is the path loss exponent, d_0 is the normalization distance, and d_{ij} is the distance between transmitter j and receiver i .

For the two-transmitter case, the eigenvalues of the matrix F are $\pm \rho \sqrt{h_{12}h_{21}/h_{11}h_{22}}$, where h_{ij} is given in (7). Hence,

$$\sigma_F = \rho \sqrt{h_{12}h_{21}/h_{11}h_{22}} < 1$$

leads to

$$\frac{d_{12}d_{21}}{d_{11}d_{22}} > \rho^{\frac{2}{\gamma}}. \quad (8)$$

Let $\mathbf{t}_i \in \mathbb{R}^2$ be transmitter i 's position, $i \in \{1, 2\}$, $\mathbf{r}_i \in \mathbb{R}^2$ be receiver i 's position, and let

$$d_i \triangleq \|\mathbf{t}_i - \mathbf{r}_i\|; \quad \tilde{d}_i \triangleq \|\mathbf{t}_i - \mathbf{r}_{3-i}\| \quad (9)$$

be the distances of the desired links and the interfering “links”, respectively. Also, let $\hat{\rho} \triangleq \rho^{\frac{1}{\gamma}}$. Then the convergence condition in (8) can be rewritten as

$$\frac{\tilde{d}_1 \tilde{d}_2}{d_1 d_2} > \hat{\rho}^2, \quad (10)$$

Our goal is to find out what constraints on their placement the two transmitters (Tx1, Tx2) have to satisfy in order to guarantee that the distributed power control algorithm converges, given the locations of the receivers.

First, letting

$$b(x, y) \triangleq \hat{\rho} \frac{x}{y}, \quad (11)$$

the convergence condition is equivalent to

$$b(d_1, \tilde{d}_1) b(d_2, \tilde{d}_2) < 1, \quad (12)$$

which shows the symmetry in the two links.

By Apollonius's definition of a circle [15], $\{\mathbf{t}_i : b(d_i, \tilde{d}_i) = c\}$, where c is a constant, defines a circle if the \mathbf{r}_i 's are given. Hence, (12) means that if \mathbf{t}_1 sits on the circle defined by $b(d_1, \tilde{d}_1) = c$, \mathbf{t}_2 must be in the region $\{\mathbf{t}_2 : b(d_2, \tilde{d}_2) < c^{-1}\}$ which is either inside or outside the circle $b(d_2, \tilde{d}_2) = c^{-1}$ depending on the value of c , and vice versa.

Now, assume that $\mathbf{r}_1 = (-a, 0)$ and $\mathbf{r}_2 = (a, 0)$ so that the distance between the two receivers is $2a$. Fixing the two receivers at the given locations means

$$d_1 \triangleq \|\mathbf{t}_1 - (-a, 0)\|, \quad d_2 \triangleq \|\mathbf{t}_2 - (a, 0)\|; \quad \tilde{d}_1 \triangleq \|\mathbf{t}_1 - (a, 0)\|, \quad \tilde{d}_2 \triangleq \|\mathbf{t}_2 - (-a, 0)\|. \quad (13)$$

Note that $b(d_1, \tilde{d}_1) = c$ is equivalent to $\mathbf{t}_1 \in \mathcal{C}_1(c)$, where $\mathcal{C}_1(c)$ is the circle

$$\mathcal{C}_1(c) = \{x, y \in \mathbb{R} : (x - x_1(c))^2 + y^2 = R_1^2(c)\}, \quad (14)$$

with $x_1(c) = a \frac{c^2 + \hat{\rho}^2}{c^2 - \hat{\rho}^2}$, $R_1(c) = \frac{2ac\hat{\rho}}{|\hat{\rho}^2 - c^2|}$.

Similarly, $b(d_2, \tilde{d}_2) = c^{-1}$ defines another circle $\mathcal{C}_2(c)$ given by

$$\mathcal{C}_2(c) = \{x, y \in \mathbb{R} : (x - x_2(c))^2 + y^2 = R_2^2(c)\}, \quad (15)$$

with $x_2(c) = a \frac{c^2 + \hat{\rho}^{-2}}{c^2 - \hat{\rho}^{-2}}$, $R_2(c) = \frac{2ac\hat{\rho}^{-1}}{|\hat{\rho}^{-2} - c^2|}$.

With the above setup, we have the following lemma, which describes the constraints on the placement of two transmitters given that the locations of two receivers are known.

Lemma 1. *Given \mathbf{r}_1 and \mathbf{r}_2 , if $\mathbf{t}_1 \in \mathcal{C}_1(c)$, where $c > \hat{\rho}^{-1}$, then $\mathbf{t}_2 \in \mathcal{D}_2$, where \mathcal{D}_2 is the disk enclosed by \mathcal{C}_2 ; conversely, if $\mathbf{t}_1 \in \mathcal{C}_1(c)$, where $c < \hat{\rho}^{-1}$, then $\mathbf{t}_2 \in \mathcal{D}_2^c$, where c indicates set complement, i.e., $\mathcal{D}_2^c = \mathbb{R}^2 \setminus \mathcal{D}_2$.*

Proof

The proof is straightforward from the definitions of the two circles $\mathcal{C}_1(c)$ and $\mathcal{C}_2(c)$ and the condition in (12). Hence, it is omitted here. \square

Fig. 2 illustrates Tx2's location constraint for different $u_1 = d_1/\tilde{d}_1$. For Fig. 2(a), when Tx1 is on the dashed circle ($u_1 = 2$), the dotted region shows the region of convergence for the power control algorithm. Here, the region of convergence (ROC) is defined as the set of Tx2's locations that guarantee the convergence of the SINRs to the desired threshold for both receivers when $\mathbf{t}_1 \in \mathcal{C}_1(c)$. This case is especially interesting because Rx2 is sometimes closer to Tx1 than Rx1 but can still receive from Tx2 as long as Tx2 is inside the circle \mathcal{C}_2 . Moreover, Fig. 2(d) shows that the Tx1-Rx1 link can even *nest within* the Tx2-Rx2 link.

3.3. Möbius Transform

In Section 3.2, we have seen that for every circle $\mathcal{C}_1(c)$ on which Tx1 is located, there is a circle $\mathcal{C}_2(c)$ which serves as the boundary for Tx2's ROC. That means that there is one-to-one mapping between the circles. The Möbius transform maps generalized circles into generalized circles on the complex plane [2]. Hence it is perfectly suited to provide a connection between the circles in our results. To see this, we first quote a lemma about the Möbius transform from [2].

Lemma 2. [2] *If a Möbius transform $f: \mathbb{C} \rightarrow \mathbb{C}$, given by $\omega = f(z) = \frac{e_1 z + e_2}{e_3 z + e_4}$, has two fixpoints α and ϕ , i.e. $\alpha = f(\alpha)$, $\phi = f(\phi)$, f can be written in the normal form*

$$\frac{\omega - \alpha}{\omega - \phi} = m \frac{z - \alpha}{z - \phi}, \quad (16)$$

where $m = \frac{e_1 + e_4 - \sqrt{D}}{e_1 + e_4 + \sqrt{D}}$, $\alpha = \frac{e_1 - e_4 + \sqrt{D}}{2e_3}$, $\phi = \frac{e_1 - e_4 - \sqrt{D}}{2e_3}$, $D = (e_1 - e_4)^2 + 4e_2e_3$.

Applying the Möbius transform to the power control problem and assuming the equivalence of \mathbb{R}^2 and \mathbb{C} with $(x, y) \in \mathbb{R}^2$ and $(x + jy) \in \mathbb{C}$ denoting the same point, we have the following result:

Theorem 3. *Let $2a$ denote the distance between Rx1 and Rx2. The relationship between \mathcal{C}_1 and \mathcal{C}_2 in (14), (15) can be expressed using a Möbius transform that only depends on the*

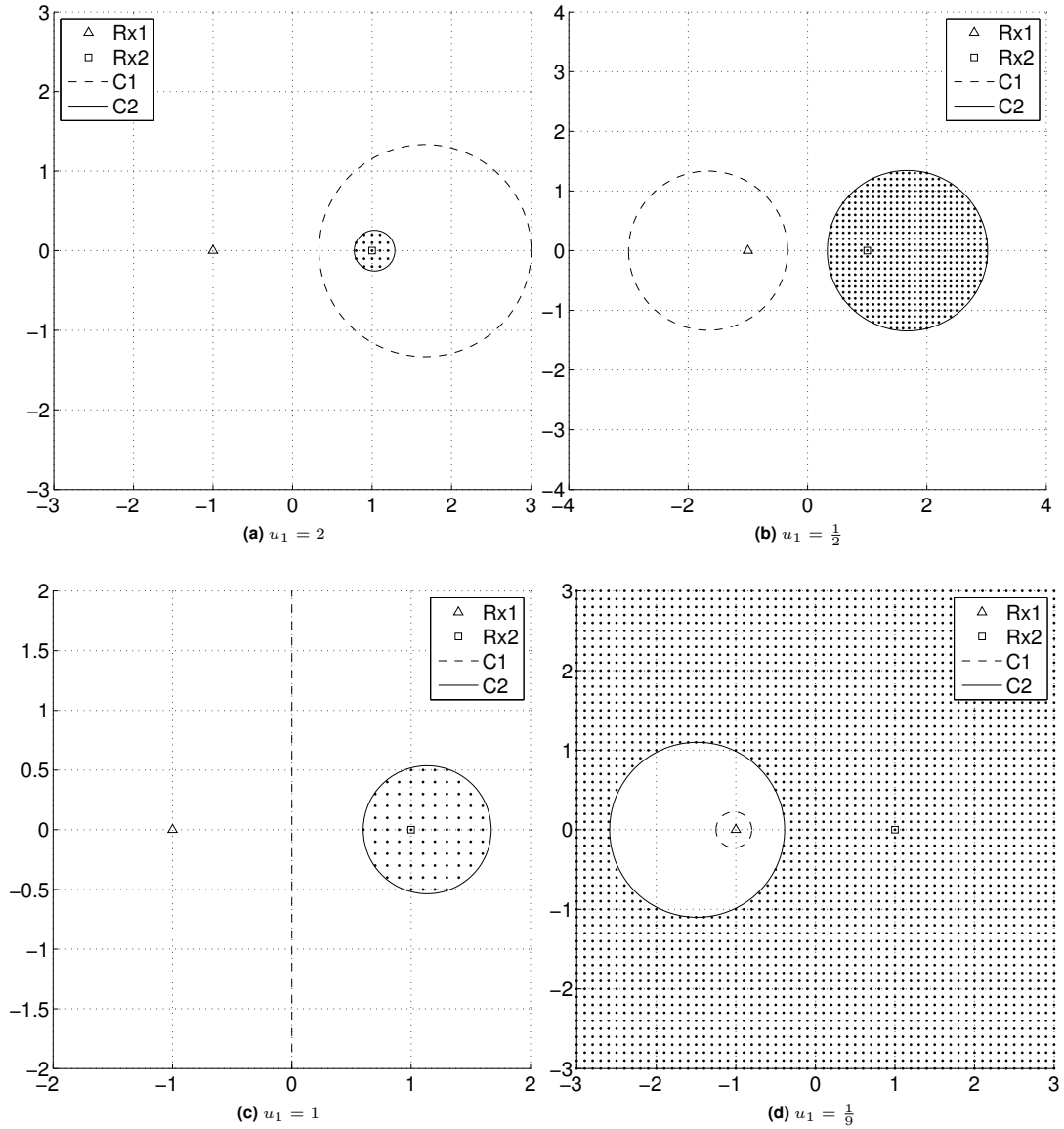


Figure 2. Tx2's ROC for different $u_1 = d_1/\tilde{d}_1$. The other parameters are $a = 1, \gamma = 4, \rho = 12$ dB.

desired SINR ρ and a :

$$f(z) = a \frac{(\hat{\rho}^2 + 1)z + (\hat{\rho}^2 - 1)a}{(\hat{\rho}^2 - 1)z + (\hat{\rho}^2 + 1)a}. \quad (17)$$

Proof

First, every point (x, y) in \mathbb{R}^2 corresponds to a point $z = x + jy \in \mathbb{C}$ whose conjugate is denoted by $\bar{z} = x - jy$. The circles \mathcal{C}_1 and \mathcal{C}_2 in (14), (15) can be represented as follows:

$$\mathcal{C}_1 : A_1 z \bar{z} + \bar{B}_1 z + B_1 \bar{z} + C_1 = 0, \quad (18)$$

$$\mathcal{C}_2 : A_2 z \bar{z} + \bar{B}_2 z + B_2 \bar{z} + C_2 = 0, \quad (19)$$

where $A_1 = c^2 \hat{\rho}^{-4} - 1$, $B_1 = \bar{B}_1 = -a(c^2 \hat{\rho}^{-4} + 1)$, $C_1 = a^2(c^2 \hat{\rho}^{-4} - 1)$; $A_2 = c^2 \hat{\rho}^4 - 1$, $B_2 = \bar{B}_2 = -a(c^2 \hat{\rho}^4 + 1)$, $C_2 = a^2(c^2 \hat{\rho}^4 - 1)$, $c > 0$.

To obtain the Möbius transform using Lemma 2, we need to identify two fixpoints of the transform and one pair of points that are mapped to each other. In (18), (19), as c goes to infinity, \mathcal{C}_1 and \mathcal{C}_2 will converge to the same point $(a, 0)$. Similarly, as c goes to zero, \mathcal{C}_1 and \mathcal{C}_2 will converge to the same point $(-a, 0)$. Therefore, $(a, 0)$, $(-a, 0)$ are two fixpoints of our Möbius transform, which are actually the locations of the two receivers. For $\forall c$, assume that $z_1 = \left(a \frac{c+\hat{\rho}}{c-\hat{\rho}}, 0\right) \in \mathcal{C}_1$ is mapped to $\omega_1 = \left(a \frac{c+\hat{\rho}^{-1}}{c-\hat{\rho}^{-1}}, 0\right) \in \mathcal{C}_2$. Inserting z_1 , ω_1 and two fixpoints into (16), we have

$$m = \frac{\omega_1 - a}{\omega_1 + a} \cdot \frac{z_1 + a}{z_1 - a}. \quad (20)$$

Inserting m back into (16), we obtain

$$\omega = f(z) = a \frac{(\hat{\rho}^2 + 1)z + (\hat{\rho}^2 - 1)a}{(\hat{\rho}^2 - 1)z + (\hat{\rho}^2 + 1)a}. \quad (21)$$

□

(21) is the Möbius transform from \mathcal{C}_2 to \mathcal{C}_1 and, conversely, $z = f^{-1}(w) = a \frac{(\hat{\rho}^2 + 1)\omega - (\hat{\rho}^2 - 1)a}{(\hat{\rho}^2 - 1)\omega - (\hat{\rho}^2 + 1)a}$ is the corresponding transform from \mathcal{C}_1 to \mathcal{C}_2 . The Möbius transform obtained here can be used as a mechanism to select concurrently active links based on the SINR requirement and the location information of the receivers. Therefore, it is very helpful for the design of MAC protocols. We will explore this in Section 5.

4. ANALYSIS OF POWER CONTROL WITH PEAK POWER CONSTRAINTS

In the previous section, we only focused on the convergence condition for power control with the assumption that there are no constraints on the transmit power. However, this is not realistic due to hardware limitations and regulations. The existing power control algorithms with peak power constraint only guarantee the convergence of the transmit powers but not for the receivers' SINRs. Moreover, the impact that peak power constraints have on wireless networks is not well understood. For example, is there a metric to quantize the convergence of the power control algorithm when peak power constraints are present?

To solve these issues, we start with the two-transmitter case where both transmitters and receivers are restricted to the real line \mathbb{R} . Then, we study power control with peak power constraints for random networks, and define a novel metric to measure the convergence of

the power control algorithm under the peak power constraint. The properties of this novel metric are analyzed in detail.

4.1. Analysis of Power Levels in Linear Networks with 2 Links

For this network, the convergence condition remains the same as in (12). As in Section 3.2, if Tx1 sits on $b(d_1, \tilde{d}_1) = c$, Tx1 is on either point $t_1 = a \frac{c-\hat{\rho}}{c+\hat{\rho}}$ or $a \frac{c+\hat{\rho}}{c-\hat{\rho}}$ for the linear network instead of a circle for two-dimensional networks. Similarly, $b(d_2, \tilde{d}_2) = c^{-1}$ defines another two points $a \frac{c\hat{\rho}-1}{c\hat{\rho}+1}$ and $a \frac{c\hat{\rho}+1}{c\hat{\rho}-1}$. If $t_1 = a \frac{c-\hat{\rho}}{c+\hat{\rho}}$ or $a \frac{c+\hat{\rho}}{c-\hat{\rho}}$, where $c > \hat{\rho}^{-1}$, then $t_2 \in (a \frac{c\hat{\rho}-1}{c\hat{\rho}+1}, a \frac{c\hat{\rho}+1}{c\hat{\rho}-1})$. Conversely, if $t_1 = a \frac{c-\hat{\rho}}{c+\hat{\rho}}$ or $a \frac{c+\hat{\rho}}{c-\hat{\rho}}$, where $c < \hat{\rho}^{-1}$, then $t_2 \in (a \frac{c\hat{\rho}+1}{c\hat{\rho}-1}, a \frac{c\hat{\rho}-1}{c\hat{\rho}+1})^c$. Similar to the ROC, define the Interval of Convergence (IOC) for linear networks. Here, let $b_1 = a \frac{c\hat{\rho}-1}{c\hat{\rho}+1}$ and $b_2 = a \frac{c\hat{\rho}+1}{c\hat{\rho}-1}$. Therefore, if $c > \hat{\rho}^{-1}$, the IOC is $\mathcal{I}_1 = (b_1, b_2)$; if $c < \hat{\rho}^{-1}$, the IOC is $\mathcal{I}_2 = (b_2, b_1)^c$. For the latter case, it means that if Tx1 and Rx1 are close enough, their link can nest inside the Tx2-Rx2 link as long as the transmit power is large enough similar to the case in Fig. 2(d).

Fig. 3 shows that the optimal power without power constraint depends on Tx2's locations given a fixed Tx1 location t_1 . The IOCs highlighted in Fig. 3 agree with the analytical intervals \mathcal{I}_1 and \mathcal{I}_2 for different scenarios. Note that the flat part of the transmit power is due to the assumption that $h_{ij} = \min \left\{ 1, \left(\frac{d_0}{d_{ij}} \right)^\gamma \right\}$ since no receiver ever gets more power than is transmitted.

Fig. 3 shows the power allocations with varied Tx2 locations for some specific locations of Tx1 and given the receivers' locations. Fig. 3(d) resembles the case in Fig. 2(d) in which a short link nests within a longer one. However, with a peak power constraint, the SINR condition may not be satisfiable even if the convergence condition is met. As a result, the IOC will shrink.

4.2. Analysis of Peak Power Constraints in Random Networks

In this subsection, two different types of networks with random node locations are studied to illustrate how the peak power constraint affects the convergence of the power control algorithm, averaged over different network topologies.

First, we define this metric to measure the convergence when there is a peak power constraint for each node in the wireless network.

Definition 4. (Convergence Probability) The convergence probability under the power constraint P_{\max} is defined as the probability that there exists a feasible power vector $P^* \leq P_{\max}$ componentwise that satisfies (2) for randomly located nodes in the network. It is denoted as $\mathcal{P}_{\text{con}}(P_{\max})$ or \mathcal{P}_{con} . For the special case where there is no power constraint, i.e., $P_{\max} = \infty$, the convergence probability is denoted as $\mathcal{P}_{\text{con}}(\infty)$.

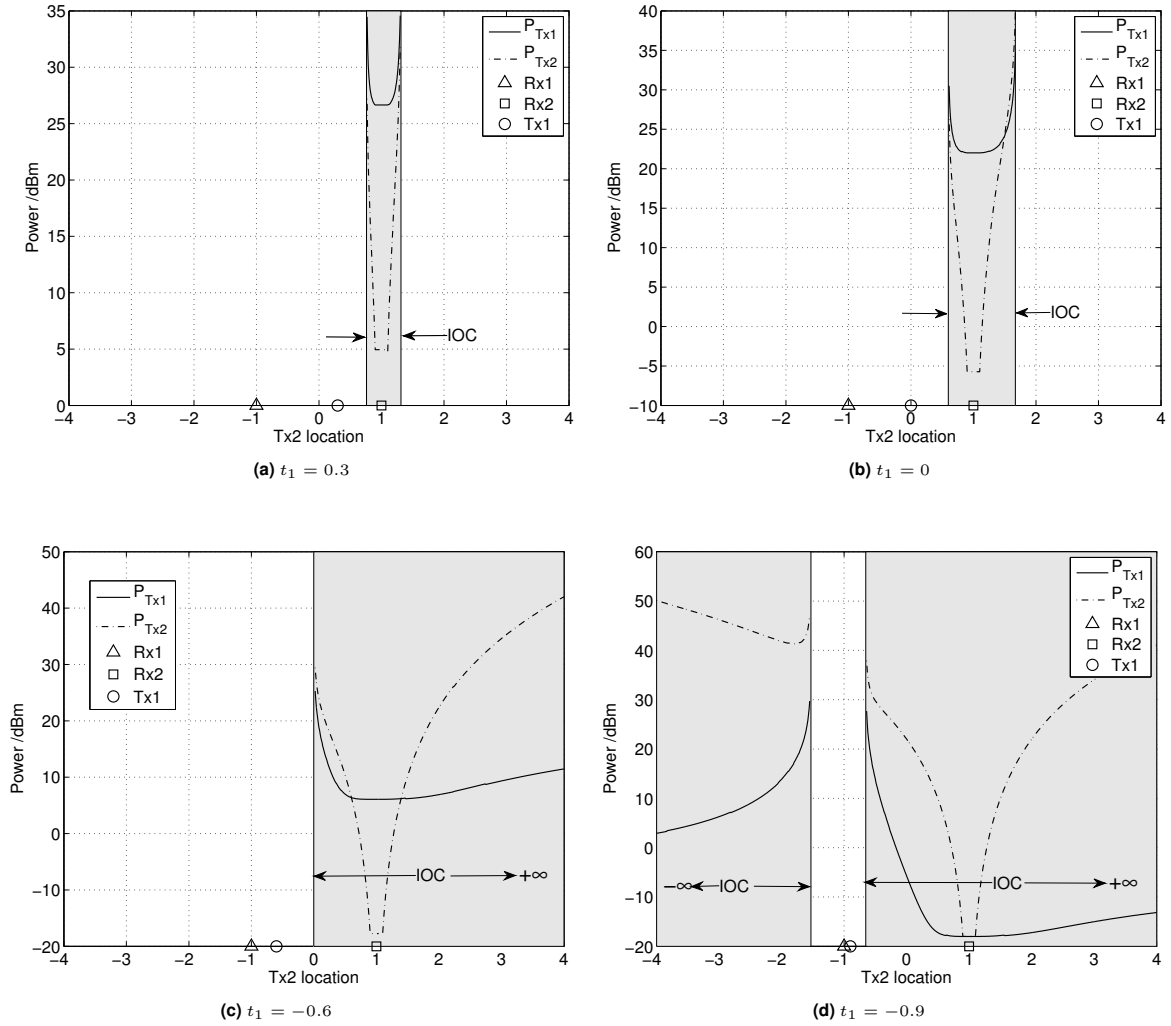


Figure 3. Optimal power for two transmitters with different Tx2 locations (the grey shadowed region indicates the IOC) for $a = 1, \gamma = 4, \rho = 12$ dB, $\eta = -30$ dBm and $d_0 = 0.1$.

The convergence probability implies both the convergence of the transmit power and the receivers' SINR to the desired threshold. $\mathcal{P}_{\text{con}}(P_{\text{max}})$ can be estimated by the fraction of realizations for which the power control algorithm converges under the power constraint P_{max} in simulation runs. The power update policy with power constraints is [11, 12]

$$P_i(k+1) = \min \left\{ \frac{\rho}{\rho_i(k)} P_i(k), P_{\text{max}} \right\}. \quad (22)$$

First, we present two general lemmas about \mathcal{P}_{con} .

Lemma 5. *The convergence probability \mathcal{P}_{con} is a non-decreasing function of the power constraint P_{max} , and its maximum is*

$$\mathcal{P}_{\text{con}}(\infty) \triangleq \mathbb{P}(\sigma_F < 1), \quad (23)$$

where σ_F is the Perron–Frobenius eigenvalue of the random matrix F defined in (4).

Proof

Let $P_{\text{max},1} < P_{\text{max},2}$, and

$$\begin{aligned} \mathcal{P}_{\text{con}}(P_{\text{max},2}) &= \mathbb{P}(\{\exists P^* \leq P_{\text{max},1} \text{ s.t. (2) holds}\} \cup \\ &\quad \{\exists P^* \text{ s.t. } P_{\text{max},1} \leq P^* \leq P_{\text{max},2} \text{ and (2) holds}\}) \end{aligned} \quad (24)$$

$$\geq \mathbb{P}(\{\exists P^* \leq P_{\text{max},1} \text{ s.t. (2) holds}\}) \quad (25)$$

$$= \mathcal{P}_{\text{con}}(P_{\text{max},1}). \quad (26)$$

Therefore, it is a non-decreasing function of P_{max} . As a result, its maximum is $\mathcal{P}_{\text{con}}(\infty)$. \square

Note that the matrix F is a random matrix due to the random node locations. Although Lemma 5 gives an expression for $\mathcal{P}_{\text{con}}(\infty)$, there is no explicit expression for \mathcal{P}_{con} in general. However, an upper bound of the convergence probability \mathcal{P}_{con} can be derived by omitting the interference in the SINR, which leads to the following lemma.

Lemma 6. *Assume that the transmitters \mathbf{t}_i and/or the receivers \mathbf{r}_i ($i \in [n]$) are randomly located within a compact set $B \subseteq \mathbb{R}^d$ ($d = 1, 2$). An upper bound of the convergence probability is given by*

$$\bar{\mathcal{P}}_{\text{con}}(P_{\text{max}}) = \mathbb{E} \left[1_{\left\{ \mathbf{t}_i, \mathbf{r}_i \in B \text{ and } \|\mathbf{t}_i - \mathbf{r}_i\| \leq \Phi^{\frac{1}{\gamma}}, \quad \forall i \in [n] \right\}} \right] \quad (27)$$

where $\Phi = \frac{P_{\text{max}} d_0^\gamma}{\rho \eta}$.

Proof

When the interference term is absent,

$$\rho_i = \frac{h_{ii} P_i}{\eta}, \quad \forall i \in [n], \quad (28)$$

with $P_i \leq P_{\text{max}}$. Therefore, $\rho_{i,\text{max}} = \frac{h_{ii} P_{\text{max}}}{\eta}$. To satisfy the convergence condition, $\rho_{i,\text{max}}$ must be greater than or equal to the desired SINR threshold ρ for any i , which leads to

$$\frac{\left(\frac{d_0}{d_{ii}}\right)^\gamma P_{\text{max}}}{\eta} \geq \rho, \quad \forall i \in [n]. \quad (29)$$

By algebraic deduction, it is easily shown that (29) is equivalent to

$$d_{ii} \leq \Phi^{\frac{1}{\gamma}}, \quad \forall i \in [n], \quad (30)$$

where $\Phi = \frac{P_{\max} d_0^\gamma}{\rho\eta}$. With $\|\mathbf{t}_i - \mathbf{r}_i\| = d_{ii}$ and the definition of the convergence probability, we obtain (27). \square

To obtain concrete results, we will discuss \mathcal{P}_{con} , $\mathcal{P}_{\text{con}}(\infty)$ and some related bounds in the following two cases.

4.2.1. One-dimensional Random Networks

Assume that Tx1 is uniformly randomly placed within the interval $[-2, 0]$ and Tx2 within $[0, 2]$, and that the two receivers are fixed in $[-1, 0]$ and $[0, 1]$ respectively. Here, $B = [-2, 2]$.

The convergence probability without peak power constraints from Lemma 5 is

$$\mathcal{P}_{\text{con}}(\infty) = \mathbb{P}(\sigma_F < 1) \quad (31)$$

$$= \mathbb{P}\left(b(d_1, \tilde{d}_1)b(d_2, \tilde{d}_2) < 1\right) \quad (32)$$

$$= \mathbb{E}_c \left[\mathbb{P}\left(b(d_2, \tilde{d}_2) < c^{-1} \mid c = b(d_1, \tilde{d}_1)\right) \right]. \quad (33)$$

Applying the results from Section 4.1, $\mathbb{P}\left(b(d_2, \tilde{d}_2) < c^{-1} \mid c = b(d_1, \tilde{d}_1)\right)$ is $\frac{|\mathcal{I}_2 \cap [0, 2]|}{|[0, 2]|}$ for $c < \hat{\rho}^{-1}$ or $\frac{|\mathcal{I}_1 \cap [0, 2]|}{|[0, 2]|}$ for $c > \hat{\rho}^{-1}$. Note that conditioning on c is equivalent to conditioning on Tx1. Since the location of Tx1 is assumed to be uniformly distributed within $[-2, 0]$, $\mathcal{P}_{\text{con}}(\infty)$ can be expressed as

$$\mathcal{P}_{\text{con}}(\infty) = \frac{1}{2} \left(\int_{c < \hat{\rho}^{-1}} \frac{|\mathcal{I}_2 \cap [0, 2]|}{|[0, 2]|} dx + \int_{c > \hat{\rho}^{-1}} \frac{|\mathcal{I}_1 \cap [0, 2]|}{|[0, 2]|} dx \right). \quad (34)$$

From Lemma 6, an upper bound of the convergence probability is

$$\bar{\mathcal{P}}_{\text{con}} = \left(\frac{1}{2} \int_{|x+1| \leq \min\{1, \Phi^{\frac{1}{\gamma}}\}} dx \right) \cdot \left(\frac{1}{2} \int_{|x-1| \leq \min\{1, \Phi^{\frac{1}{\gamma}}\}} dx \right). \quad (35)$$

Basic integration results in

$$\bar{\mathcal{P}}_{\text{con}} = \min \left\{ 1, \Phi^{\frac{2}{\gamma}} \right\}. \quad (36)$$

Fig. 4 illustrates how the convergence probability \mathcal{P}_{con} varies with the peak power constraint P_{\max} . The theoretical upper bound (36) is also given in Fig. 4(a). It can be seen that for small P_{\max} , the convergence probability increases almost quadratically with

P_{\max} (in dB). This region can be considered as power-limited or noise-limited since the power is so low that mainly the noise level limits the convergence. On the other hand, the convergence probability converges to a maximum asymptotically with increasing power constraint. That means the noise ceases to be a limiting factor, and the convergence probability becomes limited only by node locations, or, in other words, the interference. In this interference-limited regime, only the relative powers matter. By integrating (34) using the same parameters as in Fig. 4, we obtain $\mathcal{P}_{\text{con}}(\infty) \approx 0.93$. There is a small gap between the noise-limited and interference-limited regions as shown in Fig. 4(a), where both noise and interference play a significant role. Note that in the noise-limited regime, the upper bound $\bar{\mathcal{P}}_{\text{con}}$ is a good approximation for \mathcal{P}_{con} while \mathcal{P}_{con} coincides with $\mathcal{P}_{\text{con}}(\infty)$ in the interference-limited regime. As a result, $\min\{\bar{\mathcal{P}}_{\text{con}}, \mathcal{P}_{\text{con}}(\infty)\}$ serves as a tight upper bound and close approximation of the convergence probability \mathcal{P}_{con} .

Fig. 4(b) illustrates how the various noise levels affect the convergence probability curves. The noise-limited curves shift left as the noise level decreases while the convergence probability curves approach the same maximum \mathcal{P}_{con} , as expected.

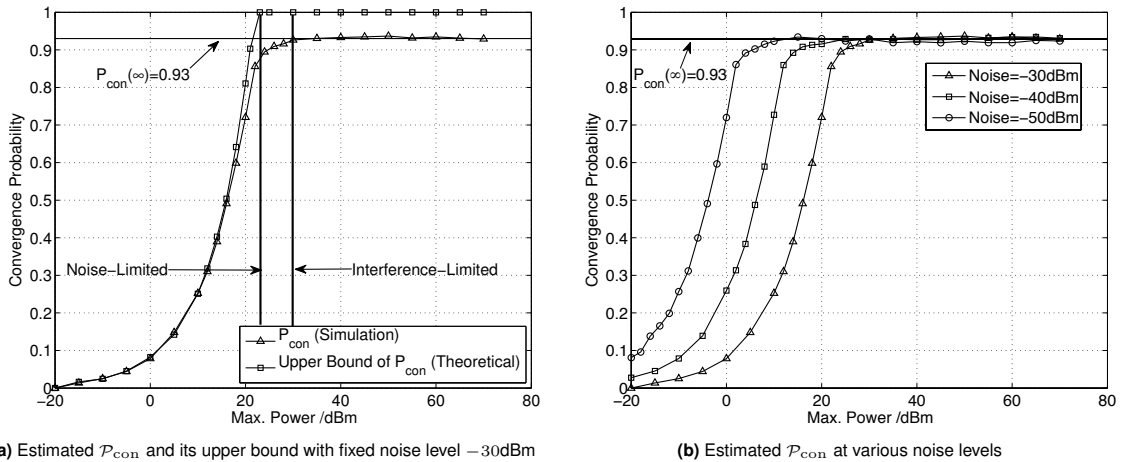


Figure 4. Estimated convergence probability \mathcal{P}_{con} vs. power constraint in linear random network with 10000 realizations for $a = 1, \gamma = 4, \rho = 12$ dB.

4.2.2. Two-Dimensional Random Networks

Consider a binomial bipolar network (BBN) where receivers form a binomial point process (BPP) [16, 17] with n receivers within $B = [0, l]^2 \subset \mathbb{R}^2$, and each receiver has a dedicated transmitter randomly located around it with deterministic constant link distances R . Therefore, there are n links in total.

Fig. 5(a) shows the estimated convergence probability from simulation with and without power constraints in a BBN. It is seen that the convergence probability decreases greatly

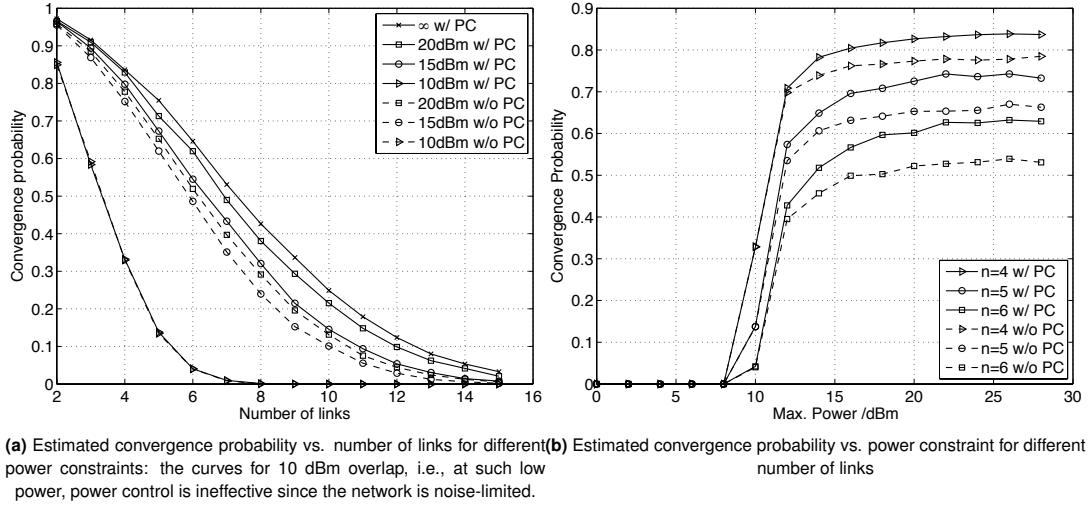


Figure 5. Comparison of estimated convergence probability in binomial bipolar network with 10000 realizations for $\gamma = 4$, $\rho = 12$ dB, $R = 0.5$, $\eta = -30$ dBm, $B = [0, 10]^2$, $d_0 = 0.1$.

as the number of links n increases. Also, for power constraints greater than 20 dBm, the convergence probability is almost the same as without power constraint. A reduction in the peak power may however have a drastic effect on the convergence probability. For comparison, also plotted are the cases without power control in which all transmitters use the maximum power. The cases without power control are illustrated in dashed lines. As seen, the convergence probability for the cases without power control is smaller than those with power control except for the case in which the power constraint is 10 dBm. Fig. 5(b) illustrates how the convergence probability varies with different power constraints for a fixed number of links. The solid lines are for the cases with power control while the dashed lines without power control. Again, power control can improve the convergence probability as illustrated. The abrupt transition starting at 10 dBm comes from the assumption of a fixed transmitter-receiver distance R . Since the convergence requires that $\rho_i = \frac{h_{ii}P_i}{\sum_{i \neq j} h_{ij}P_j + \eta} \geq \rho$, omitting the interference term in the denominator we have

$$P_i \geq \rho\eta/h_{ii} = \rho\eta \left(\frac{R}{d_0} \right)^\gamma. \quad (37)$$

Therefore, the minimal power level required depends on the desired SINR, the noise level, and the channel gain even if the convergence condition is satisfied without power constraint. By inserting the parameters into the right side of (37), it happens to be around 10 dBm, which explains why there is an abrupt transition of the convergence probability around 10 dBm. It also explains why the convergence probability curves are the same with or without power control for the case with power constraint 10 dBm. Besides, the convergence

probabilities depend on the number of links. More links will cause more mutual interference and therefore lower the convergence probability.

Their maxima are $\mathcal{P}_{\text{con}}(\infty)$, which are computable in theory from (23):

$$\mathcal{P}_{\text{con}}(\infty) = \mathbb{E}_{\mathbf{r}_1, \mathbf{r}_2, \dots, \mathbf{r}_n} [\mathbb{P}(\sigma_F < 1 \mid \mathbf{r}_1, \mathbf{r}_2, \dots, \mathbf{r}_n)] \quad (38)$$

$$= \mathbb{E}_{\mathbf{r}_1, \mathbf{r}_2, \dots, \mathbf{r}_n} \left[\underbrace{\int_{\mathbb{R}^2} \cdots \int_{\mathbb{R}^2}}_n 1_{\{\sigma_F < 1\}} \prod_{i=1}^n f(\mathbf{t}_i \mid \mathbf{r}_i) d\mathbf{t}_1 \cdots d\mathbf{t}_n \right], \quad (39)$$

$$= \mathbb{E}_{\mathbf{r}_1, \mathbf{r}_2, \dots, \mathbf{r}_n} \left[\left(\frac{1}{2\pi} \right)^n \underbrace{\int_0^{2\pi} \cdots \int_0^{2\pi}}_n 1_{\{\sigma_F < 1\}} d\theta_1 \cdots d\theta_n \right], \quad (40)$$

where $f(\mathbf{t}_i \mid \mathbf{r}_i)^*$ is the probability density function (PDF) of the transmitter i conditional on receiver i and (40) is the result for \mathbf{t}_i in polar coordinates.

There is no closed-form expression for $\mathcal{P}_{\text{con}}(\infty)$ for general n . For $n = 2$, we have the following proposition.

Proposition 1. For $n = 2$, given that $\rho > 0$ and $R_0 = R \left(1 + \rho^{\frac{1}{\gamma}}\right) < l$, $\mathcal{P}_{\text{con}}(\infty)$ is lower bounded by

$$\underline{\mathcal{P}}_{\text{con}}(\infty) = 1 - \left(\frac{\pi R_0^2}{l^2} - \frac{8R_0^3}{3l^3} + \frac{R_0^4}{2l^4} \right). \quad (41)$$

The proof is given in the appendix. Since $R = 0.5$ and $\rho = 12$ dB in simulation, these conditions $\rho > 0$ and $R_0 < l$ can be guaranteed. Inserting the same parameters as in simulations, the theoretical value of $\underline{\mathcal{P}}_{\text{con}}(\infty)$ turns out to be 0.94 while the estimated $\mathcal{P}_{\text{con}}(\infty)$ in simulation is about 0.97. Hence, (41) serves as a tight lower bound and close approximation for $\mathcal{P}_{\text{con}}(\infty)$ for $n = 2$.

Remark.

- The convergence probability is a novel metric defined to describe the influence of the peak power constraint on the convergence of the power control algorithm and has the case without peak power constraint as a special case. It has a close connection with the standard metric outage probability. The convergence probability without peak power constraint can be considered as the probability that there is no outage for any link in a wireless system with n interfering links after the power control algorithm converges.

*For BPP with fixed link distance, the pdf does not exist. However, the integral can be evaluated by assuming that the Tx is located on a thin annulus around the Rx of width ϵ , and then letting ϵ go to zero.

That is,

$$\mathcal{P}_{\text{con}}(\infty) = \prod_{i=1}^n (1 - p_{i,\text{outage}}), \quad (42)$$

where $p_{i,\text{outage}}$ is the outage probability for link i . Hence, the convergence probability can also be used as a metric for system design.

5. MÖBIUS MAC SCHEME

5.1. Introduction and Model Description

Based on the observations from the Möbius transform and the analysis of the peak power constraints, we next propose a novel MAC scheme, called Möbius MAC scheme, to schedule links in pairs instead of individually. To illustrate this concept of scheduling in pairs, we consider two-tier networks that consist of two type of links, long links with link distance l_1 and short links with link distance $l_2 < l_1$. For the long links, n points are chosen to form a BPP within the region $B = [0, l]^2 \subset \mathbb{R}^2$. Each point out of n points serves as the midpoint of two other points (one for transmitter and the other for receiver) that are separated by distance l_1 ; the orientation of the axis of the two points is uniformly chosen. The short links are placed in a similar way but have distance l_2 . Assume long links have link index $i \in \{0, 1, \dots, n-1\}$ and short links have $j \in \{n, n+1, \dots, 2n-1\}$. Such a network model can be applied to both heterogeneous networks and cognitive networks as will be discussed in Section 6. One realization of the links is illustrated in Fig. 6.

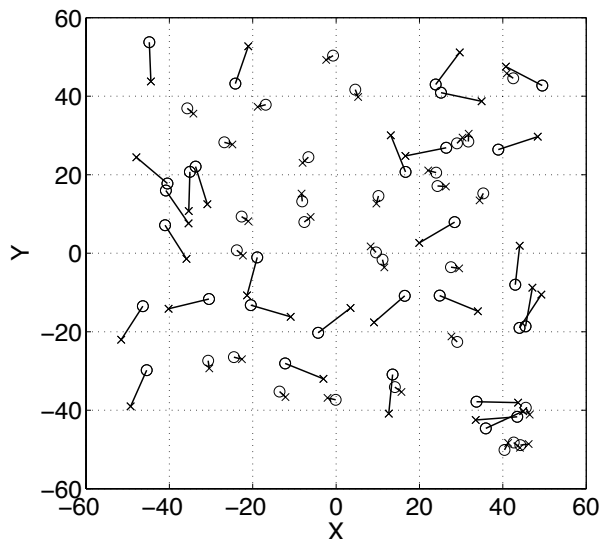


Figure 6. Illustration of a wireless network consisting of long and short links with $l_1 = 10$ and $l_2 = 2$ where the crosses indicate the transmitters, and the circles the receivers.

5.2. Description of MAC Scheme

The Möbius MAC scheme operates in two stages: first the long links are scheduled using the power control algorithm with peak power constraints, and next when the set of scheduled long links is known, the short links are scheduled to be associated with their "nearest" long links if the condition developed in the previous sections is satisfied. By doing so, the short links will team up with the long links and be scheduled to be active concurrently if possible, which can improve the spatial reuse greatly. The detailed description of the Möbius MAC scheme is as follows:

Algorithm 1 Möbius MAC scheme

- 1: The distributed power control algorithm with peak power constraint in (45) for a given set of n long links with initial power $P_i(0) = \rho\eta/h_{ii}$ is run;
 - 2: If long link i 's power $P_i(k) \geq p_{i,\max}$ in (43), link i is shut down immediately; the algorithm is run until the SINRs for the remaining long links satisfy the condition $\|\boldsymbol{\rho}(k) - \boldsymbol{\rho}^L\|_\infty \leq \epsilon\rho^L$ (ρ^L is given in (46)) for a given ϵ or the number of iterations k is greater than the maximal number of iterations k_{\max} ; $j = n$.
 - 3: The short link j is paired up with the long link whose receiver is closest to the transmitter of the short link, i.e., i . If the link pairs (i, j) can satisfy the constraint from Lemma 1, the short link gets assignment of its transmit power as $P_j = \min\left(\frac{P_i h_{ii}}{h_{ij}} \left(\frac{1}{\rho} - \frac{1}{\rho^L}\right), \rho^S \frac{P_i h_{ji} + \eta}{h_{jj}}\right)$, (ρ^S is given in (51)); else P_j is set to 0; $j \leftarrow j + 1$.
 - 4: **if** $j = 2n$ **end**, **else go to** 3
-

As specified in Algorithm 1, the long links are scheduled first. Based on the analysis of Section 4 and in [18], it is beneficial to use an adjusted peak power constraint in the power control algorithm with peak power constraint with the form in (22). Here, instead of using a fixed peak power constraint P_{\max} as in (22), we choose

$$p_{i,\max} = \frac{\beta\rho\eta}{h_{ii}}, \quad (43)$$

where $p_{i,\max}$ is the peak power constraint for transmitter i and $\beta > 1$ is a parameter that adjusts the dynamic range of the peak power constraint. The reason why the peak power constraint in (43) is chosen is because under this constraint the interference at the receiver for a scheduled link can be bounded. To see that, assuming that the transmit power of transmitter i is $p_{i,\max}$, we have for the SINR at its receiver

$$\rho_i = \frac{p_{i,\max} h_{ii}}{I_i + \eta} \geq \rho, \quad (44)$$

which leads to $I_i \leq (\beta - 1)\eta$ after inserting (43) into (44), where I_i is the interference at receiver i . In cellular systems, $\beta' = \beta - 1$ is the upper bound for the Interference over Thermal (IoT) ratio [19], which is a critical parameter for system design and analysis. Hence, we can choose the parameter β based on the system requirement. All the scheduled links are guaranteed that their interference is bounded and therefore achieve the required performance. In summary, the n long links are first scheduled based on the power control algorithm with peak power constraint

$$P_i(k+1) = \min \left\{ \frac{\rho^L}{\rho_i(k)} P_i(k), p_{i,\max} \right\}, \quad (45)$$

with

$$\rho^L = \rho(1 + \delta^L), \quad (46)$$

and initial power $P_i(0) = \rho\eta/h_{ii}$, in which $h_{ii} = l_1^{-\gamma}$ from (7) is the channel power gain between the transmitter and receiver of the long link i . Note that the positive parameter $\delta^L \ll 1$ is used to provide protection for long links from the interference from the short links that are going to be scheduled next. If any long-link's transmit power is greater than or equal to $p_{i,\max}$, that link is shut down immediately. The distributed power control algorithm is run until the SINRs for the remaining links converge to a small range around ρ^L or the number of iterations reaches to the maximal iteration threshold. In other words, the long links "sacrifice" a little in terms of transmit power (larger SINR needs higher transmit power) in order to enable the short links to be scheduled.

Let $m \leq n$ denote the number of scheduled long links out of n from the first stage. Next, we want to know how many short links out of n can be scheduled together since it has been illustrated that link nesting is possible in Section 3. The short link is made to pair up with the long link whose receiver is nearest to the transmitter of the short link. Also, assume that all receivers have the location information of their associated transmitter. In this stage, if the transmitter of the short link is within the region given in Lemma 1, a proper transmit power for the short link is assigned in a way that (1) the SINR of the long link will *not* decrease from around ρ^L to being below the desired SINR threshold ρ ; (2) the SINR of the short link should be above the SINR threshold ρ if possible.

Now, a suboptimal transmit power for the short links is derived in the following way. Ideally, any scheduled long link is supposed to satisfy

$$\frac{P_i h_{ii}}{I_i + \eta} = \rho^L, \quad (47)$$

where P_i is the transmit power for transmitter i in the long link, and I_i is the interference at the receiver i of the long link from other scheduled long links. After the short links are scheduled, we need to guarantee that

$$\frac{P_i h_{ii}}{I_i + \eta + P_j h_{ij} + \tilde{I}_i} \geq \rho, \quad (48)$$

where P_j is the transmit power for the transmitter j in the short link that is paired up with the long link i , h_{ij} is the channel power gain from short-link's transmitter j to long-link's receiver i , and \tilde{I}_i is the interference at the long link's receiver i caused by other short-link's transmitters except short-link's transmitter j . Note that there can be multiple short links that pair up with one long link. Omitting \tilde{I}_i in (48) and combining (47) and (48), an upper bound of P_j is obtained:

$$P_j \leq \frac{P_i h_{ii}}{h_{ij}} \left(\frac{1}{\rho} - \frac{1}{\rho^L} \right). \quad (49)$$

On the other hand, in order to guarantee the SINR of the scheduled short links, we need

$$\frac{P_j h_{jj}}{P_i h_{ji} + \eta + I_j} \geq \rho^S, \quad (50)$$

where

$$\rho^S = \rho (1 + \delta^S), \quad (51)$$

in which $0 < \delta^S \ll 1$ is the margin used to protect short links from falling below the SINR threshold ρ , and h_{ji} is the channel power gain from long-link's transmitter i to short-link's receiver j , $h_{jj} = l_2^{-\gamma}$ is the channel power gain between the transmitter and receiver of the short link, and I_j is the total interference at the short link's receiver j from other links except the long-link's transmitter i . Omitting I_j , (50) leads to a lower bound of P_j :

$$P_j \geq \rho^S \frac{P_i h_{ji} + \eta}{h_{jj}}. \quad (52)$$

Hence, if $\rho^S \frac{P_i h_{ji} + \eta}{h_{jj}} \leq \frac{P_i h_{ii}}{h_{ij}} \left(\frac{1}{\rho} - \frac{1}{\rho^L} \right)$, set $P_j = \rho^S \frac{P_i h_{ji} + \eta}{h_{jj}}$ and both SINRs for the long and short links can be above the threshold; if $\rho^S \frac{P_i h_{ji} + \eta}{h_{jj}} > \frac{P_i h_{ii}}{h_{ij}} \left(\frac{1}{\rho} - \frac{1}{\rho^L} \right)$, set $P_j = \frac{P_i h_{ii}}{h_{ij}} \left(\frac{1}{\rho} - \frac{1}{\rho^L} \right)$ and the SINR of the long link can be guaranteed while the SINR of the short link may be below the threshold but make the "best effort".

5.3. Performance Evaluation

For the purpose of comparison, we use the CSMA scheme implemented as follows: if a receiver's interference power level is smaller than a threshold, the receiver sends a feedback

signal to its transmitter to set the transmit power to be

$$P_i = \frac{(1 + \delta) \rho \eta}{h_{ii}}, \quad (53)$$

where $0 < \delta \ll 1$ serves as a marginal protection to tolerate interference from other links; otherwise, it is impossible to satisfy the receiver i 's SINR. The CSMA scheme is described in detail in Algorithm 2.

Algorithm 2 CSMA

- 1: A random timer for each link among a total of n short links and n long links is assigned;
 $k = 0$
 - 2: **if** transmitter i 's timer expires, receiver i calculates its received power $P_{r,i}$. If the power level $P_{r,i} < P_0$, where $P_0 = (1 + \delta) \eta$, link i can transmit with power given by (53). Link i is then admitted into the subset of links scheduled. $k = k + 1$
 - 3: Wait for next timer expiration and **if** $k < n$ **go to** 2
 - 4: **if** $k = n$ **end**
-

The key metrics for the MAC scheme are (1) how many links can be scheduled successfully in total? (2) how many long and short links can be scheduled, respectively? In order to quantify the performance of the MAC schemes, we use the *transport density* as the performance metric as used in [18] to merge the link distance and the number of scheduled links into one metric. For clarity, we restate the definition of transport density as follows:

Definition 7. (Transport Density) The transport density is defined as the sum of the products of bits and the distances of all scheduled links whose SINR satisfies $\|\rho(k) - \rho\|_\infty \leq \epsilon$, averaged over the network realizations. It is denoted as T . Assume that all n links in a wireless network are located within a $l \times l$ region and within a time slot, a link will carry the same number of bits (W) regardless of its length as long as it can be scheduled successfully, *i.e.*, its SINR requirement can be satisfied. Then, the transport density is

$$T = \frac{W}{l^2} \mathbb{E} \left[\sum_{i=1}^n d_{ii} 1_{\{|\rho_i(k) - \rho| \leq \epsilon\}} \right],$$

where 1_A is the indicator function and d_{ii} is the link distance of link i .

Its unit is bits \cdot m/m². Note that $\rho(k) \rightarrow \rho$ can only be achieved in the limit as $k \rightarrow \infty$. Therefore, it is reasonable to loosen the convergence condition to be that the error of SINRs is within some range $0 < \epsilon \ll 1$ of the target SINR.

This metric is a precise indicator of a network's capacity. For link scheduling, maximizing the transport density is more meaningful than maximizing the number of successfully scheduled links as in [20] since a longer link contributes more to the transport density than a shorter link.

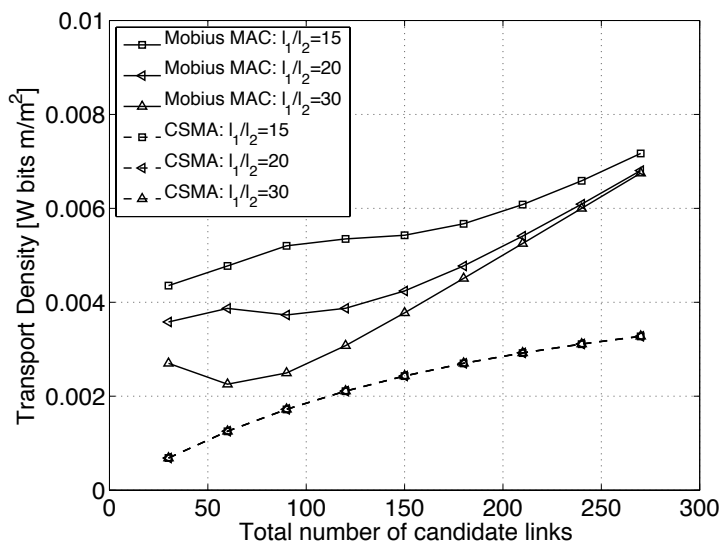


Figure 7. Transport density of scheduled links vs the total number of candidate long/short link with different long link distances: $l_1 = 15, 20, 30$, $l_2 = 1$, $B = [0, 200]^2$, $\gamma = 4$, $\rho = 11$ dB, $\delta = \delta^S = 0.09$, $\delta^L = 0.009$, $\beta = 50$, $\eta = -60$ dBm, $\epsilon = 1\%$, $k_{\max} = 30$.

Fig. 7 shows the transport density of the scheduled links as a function of the total number of candidate long/short link number for the different long/short link distance ratios. As seen, the transport density for Möbius MAC is roughly twice as that of CSMA. In general, Möbius MAC always has better performance than CSMA in terms of transport density. The reason is that Möbius MAC schedules long links first and then short links while CSMA implicitly gives preference to the short links. The reason is that the long links are easily prohibited from transmitting since they would cause strong interference to others or getting interfered by others. This disparity could lead to a fairness problem in scheduling. Also, as the long/short link distance ratio decreases, the transport density using Möbius MAC is getting larger. On the other hand, the transport density of CSMA does not change with the long/short link distance ratio due to the fact that all the long links are prohibited from transmitting by CSMA.

In general, Möbius MAC scheme can provide relatively fair scheduling or sometimes gives preference to long links while CSMA has difficulty in scheduling long links since they are easily prohibited from transmitting by short links. Moreover, the QoS performance of the scheduled links in terms of transport density by the Möbius MAC scheme is also much better than that by CSMA.

6. APPLICATIONS

In this section, we will highlight two applications of our analysis and MAC scheme. One is for cognitive radio networks while the other for heterogeneous networks.

6.1. Application to Cognitive Radio Networks

The analysis of power levels in linear networks with two transmitters in Section 4.1 provides a new perspective on the spatial reuse of cognitive radios that share the spectrum with the primary users through spatial separation [21, 22].

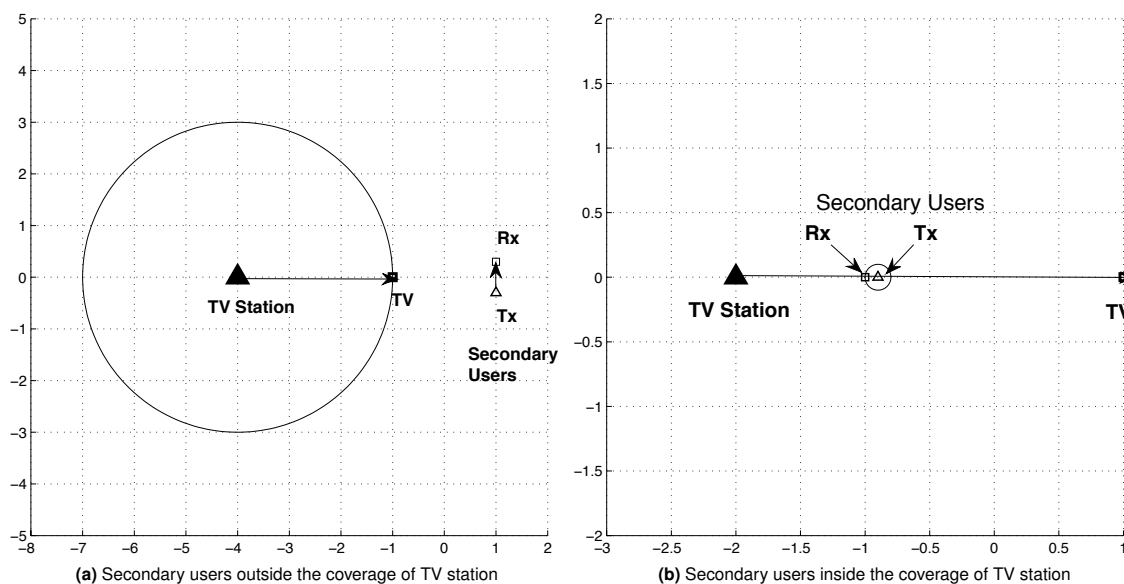


Figure 8. Illustrations of spectrum sharing of a cognitive radio network with a TV broadcast system.

One example is a cognitive radio network sharing spectrum with a TV broadcast system. Usually, the secondary users' locations are assumed to be outside the coverage of the TV station as illustrated in Fig. 8(a). However, as analyzed in Sections 3.2 and 4.1, this does not have to be the case. Assume that the power constraint for the TV station is $P_{TV,max} = 50$ dBm and that for the secondary users is $P_{S,max} = 20$ dBm. Fig. 9 shows the IOC of the TV station. The IOC bounded by the grey rectangle is the case with power constraints. Although the IOC is decreased due to the power constraints, the cognitive radio network can still find a feasible power allocation as long as the TV station is located within the power-constrained IOC. Therefore, the secondary users can still be located within the coverage of the TV station while maintaining their SINR above the threshold. Fig. 8(b) illustrates how this case looks in contrast to the traditional layout in Fig. 8(a). As shown, only the secondary users

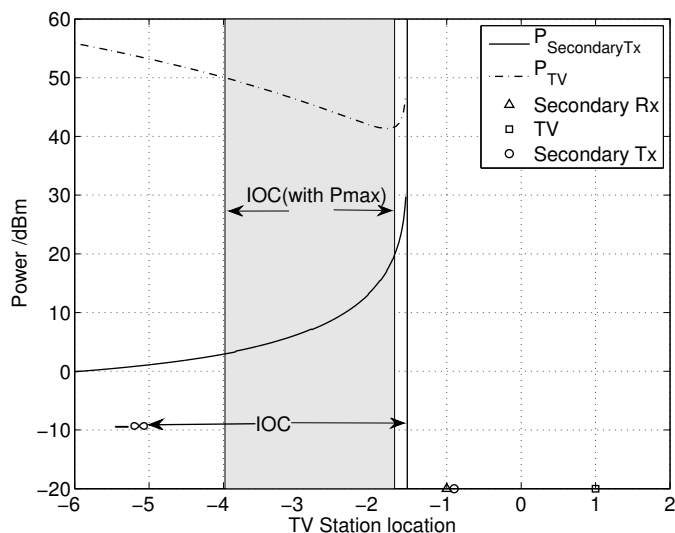


Figure 9. The IOC for TV station with or without power constraints (the grey shadowed region indicates the IOC with power constraints) for $\alpha = 1$, $\gamma = 4$, $\rho = 12$ dB, $P_{TV,max} = 50$ dBm, $P_{S,max} = 20$ dBm.

with small link distances can be tolerated within the coverage of the TV station. Short links offer the dual benefits of higher quality links and improved spatial reuse.

The Möbius MAC scheme can readily be applied to cognitive radio networks. The primary users are scheduled first as the long links while the secondary users pair up with the "nearest" primary user and are scheduled jointly according to the criterion. The primary users' performance is always guaranteed while the secondary users "squeeze" in and make best-effort delivery whenever possible.

6.2. Application to Heterogeneous Cellular Networks

Another example is the concept of femtocells [23]. Femtocell deployment can improve indoor voice and data reception with the advantages of short range, low cost and low power. In this subsection, we focus on macro-femto heterogeneous networks. As illustrated in Figure 10, this is the scenario considered where there is a femto-cell inside a home to which only the owner has access while the user outside is barred from accessing the femto base station even if he/she is close to it. As a result, the interference caused by the femto base stations to the outside user can be severe. On the other hand, the user inside the home may experience interference from the macro base station due to its strong downlink signal strength. In general, femto networks need interference coordination via resource partitioning across base stations to manage inter-cell interference [24]. Such resource partitioning can be performed in the time domain, frequency domain, or spatial domain. However, with the geometric analysis in our paper, it is possible to use the resources in a more aggressive way,

i.e., the links between macro base station and the outside user and between the femto base station and its owner can share the same spectrum at the same time without having to resort to spatial partitioning. Lemma 1 can serve as criterion for the macro-femto networks to see if they can coexist. If the geometric conditions in Lemma 1 are satisfied, the macro base station can serve as a centralized controller and choose the transmit powers for itself and femto base station that can satisfy their SINR conditions ρ^L and ρ^S respectively without going through the distributed power control algorithm. If the transmit powers exceed the peak power constraint for macro base station or femto base station, they need to be allocated to different resources and cannot share the spectrum with each other even if the geometric condition is satisfied in Lemma 1.

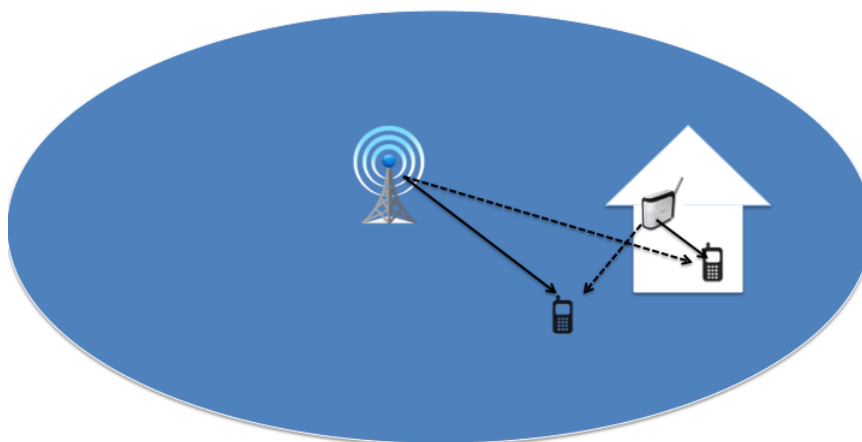


Figure 10. A heterogeneous network consisting of a macro and a femto base station with two mobile users where the solid lines indicate the communication links and the dashed lines the interference.

7. CONCLUDING REMARKS

In this paper, we first presented a geometric analysis of the power control convergence condition. A novel analytical tool, the Möbius transform, was used to analyze the convergence conditions. The effect of peak power constraints was analyzed in detail to illustrate its influence on random networks. A novel metric, the convergence probability, has been used to study the impact of the peak power constraints.

In general, the power constraint makes the power control problem more complex. Our research provides insight into the design of MAC protocols with dynamic power control under peak power constraints. A novel MAC scheme based on Möbius transform and peak power constraints has been proposed to show that link nesting is possible under peak power constraints. It works well especially in wireless networks with unequal link distances. This is important for the design and analysis of cognitive radio networks, where the secondary

users can be placed near the primary transmitter as long as the link distance of the secondary users is short enough and its transmit power is not too high, and heterogeneous networks, where the macro base stations and femto base stations are coexisting. Simulations showed that the performance of our novel MAC is twice as good as that of CSMA in terms of transport density. In summary, the MAC design combining with power control from physical layer takes full advantage of the scarce spectrum and provides new perspective on the cross-layer design in wireless network.

ACKNOWLEDGEMENT

This work was partially supported by the NSF (grants CNS 1016742 and CCF 1216407).

APPENDIX

Proof of Proposition 1

Proof

For $n = 2$,

$$\mathcal{P}_{\text{con}}(\infty) = \mathbb{E}_{\mathbf{r}_1, \mathbf{r}_2} \left[\int \int 1_{\{\|\mathbf{t}_1 - \mathbf{r}_2\| \cdot \|\mathbf{t}_2 - \mathbf{r}_1\| > R^2 \rho^{2/\gamma}\}} f(\mathbf{t}_1 | \mathbf{r}_1) f(\mathbf{t}_2 | \mathbf{r}_2) d\mathbf{t}_1 d\mathbf{t}_2 \right] \quad (54)$$

$$= \mathbb{E}_{\mathbf{r}_1, \mathbf{r}_2} \left[\left(\frac{1}{2\pi} \right)^2 \int_0^{2\pi} \int_0^{2\pi} 1_{\{\|R e^{j\theta_1} + \mathbf{r}_1 - \mathbf{r}_2\| \cdot \|R e^{j\theta_2} + \mathbf{r}_2 - \mathbf{r}_1\| > R^2 \rho^{2/\gamma}\}} d\theta_1 d\theta_2 \right] \quad (55)$$

$$= \mathbb{E}_{\mathbf{r}_1, \mathbf{r}_2} \left[\left(\frac{1}{2\pi} \right)^2 \int_0^{2\pi} \int_0^{2\pi} 1_{\{\|e^{j\theta_1} + \frac{\mathbf{r}_1 - \mathbf{r}_2}{R}\| \cdot \|e^{j\theta_2} + \frac{\mathbf{r}_2 - \mathbf{r}_1}{R}\| > \rho^{2/\gamma}\}} d\theta_1 d\theta_2 \right] \quad (56)$$

$$\stackrel{(a)}{\geq} \mathbb{E}_{\mathbf{r}_1, \mathbf{r}_2} \left[\left(\frac{1}{2\pi} \right)^2 \int_0^{2\pi} \int_0^{2\pi} 1_{\{\|\frac{\mathbf{r}_1 - \mathbf{r}_2}{R} - 1\| \cdot \|\frac{\mathbf{r}_2 - \mathbf{r}_1}{R} - 1\| > \rho^{2/\gamma}\}} d\theta_1 d\theta_2 \right] \quad (57)$$

$$= \mathbb{E}_{\mathbf{r}_1, \mathbf{r}_2} \left[1_{\{(\|\frac{\mathbf{r}_1 - \mathbf{r}_2}{R} - 1\|)^2 > \rho^{2/\gamma}\}} \right], \quad (58)$$

where (a) results from the triangle inequality. Hence, a lower bound of $\mathcal{P}_{\text{con}}(\infty)$ (denoted as $\underline{\mathcal{P}}_{\text{con}}(\infty)$) is

$$\underline{\mathcal{P}}_{\text{con}}(\infty) = \mathbb{E}_{\mathbf{r}_1, \mathbf{r}_2} \left[1_{\{(\|\frac{\mathbf{r}_1 - \mathbf{r}_2}{R} - 1\|)^2 > \rho^{2/\gamma}\}} \right]. \quad (59)$$

Letting $D = \|\mathbf{r}_1 - \mathbf{r}_2\|$,

$$\underline{\mathcal{P}}_{\text{con}}(\infty) = \mathbb{E}_D \left[1_{\{(\frac{D}{R} - 1)^2 > \rho^{2/\gamma}\}} \right]. \quad (60)$$

Note that \mathbf{r}_1 and \mathbf{r}_2 are two points that are independently and uniformly distributed over $B = [0, l]^2$. From Theorem 2.4.4 in [25], we can derive the PDF of their distance D as

$$f(d) = \begin{cases} \frac{2\pi d}{l^2} - \frac{8d^2}{l^3} + \frac{2d^3}{l^4}, & 0 \leq d \leq l \\ \frac{4d}{l^2} \left[\sin^{-1} \left(\frac{l}{d} \right) - \cos^{-1} \left(\frac{l}{d} \right) - \frac{d^2}{2l^2} - \frac{2\sqrt{d^2-l^2}}{l} - 1 \right], & l \leq d \leq \sqrt{2}l \\ 0, & \text{otherwise.} \end{cases} \quad (61)$$

Given $\rho > 0$ dB and $R_0 = R \left(1 + \rho^{\frac{1}{\gamma}} \right) < l$,

$$\mathcal{P}_{\text{con}}(\infty) = \mathbb{E}_D \left[1_{\left\{ \left(\frac{D}{R} - 1 \right)^2 > \rho^{2/\gamma} \right\}} \right] \quad (62)$$

$$= \int_{R_0}^{\infty} f(x) dx \quad (63)$$

$$= \int_{R_0}^l \left(\frac{2\pi x}{l^2} - \frac{8x^2}{l^3} + \frac{2x^3}{l^4} \right) dx \quad (64)$$

$$+ \int_l^{\sqrt{2}l} \frac{4x}{l^2} \left[\sin^{-1} \left(\frac{l}{x} \right) - \cos^{-1} \left(\frac{l}{x} \right) - \frac{x^2}{2l^2} - \frac{2\sqrt{x^2-l^2}}{l} - 1 \right] dx \quad (65)$$

$$= \pi - 3 - \left(\frac{\pi R_0^2}{l^2} - \frac{8R_0^3}{3l^3} + \frac{R_0^4}{2l^4} \right) + I_0 - I_1, \quad (66)$$

where $I_0 = \int_l^{\sqrt{2}l} \frac{4x}{l^2} \left[\sin^{-1} \left(\frac{l}{x} \right) \right] dx$, and $I_1 = \int_l^{\sqrt{2}l} \frac{4x}{l^2} \left[\cos^{-1} \left(\frac{l}{x} \right) \right] dx$. From [25], I_0 and I_1 can be calculated in terms of Gauss' hypergeometric function. By some basic calculations, we can obtain that $I_0 = 2$ and $I_1 = 2 - \pi$. Inserting I_0 and I_1 into (66), we obtain (41). \square

REFERENCES

1. Foschini G, Miljanic Z. A simple distributed autonomous power control algorithm and its convergence. *IEEE Transactions on Vehicular Technology* Nov 1993; **42**(4):641–646, doi:10.1109/25.260747.
2. Hanh LS. *Complex numbers and geometry*. The Mathematical Association of America, 1994.
3. Grandhi S, Vijayan R, Goodman D. Distributed power control in cellular radio systems. *IEEE Transactions on Communications* Feb–Apr 1994; **42**(234):226–228, doi:10.1109/TCOMM.1994.577019.
4. Zander J. Distributed cochannel interference control in cellular radio systems. *IEEE Transactions on Vehicular Technology* Aug 1992; **41**(3):305–311, doi:10.1109/25.

- 155977.
5. ElBatt T, Ephremides A. Joint scheduling and power control for wireless ad-hoc networks. *Twenty-First Annual Joint Conference of the IEEE Computer and Communications Societies (INFOCOM'02)*, vol. 2, New York, NY, USA, 2002; 976–984, doi:10.1109/INFCOM.2002.1019345.
 6. Li Y, Ephremides A. Joint scheduling, power control, and routing algorithm for ad-hoc wireless networks. *Proceedings of the 38th Annual Hawaii International Conference on System Sciences, 2005 (HICSS'05)*, Big Island, Hawaii, USA, 2005; 322b, doi:10.1109/HICSS.2005.367.
 7. Chiang M, Hande P, Lan T, Tan CW. Power control in wireless cellular networks. *Found. Trends Netw.* Apr 2008; **2**(4):381–533, doi:10.1561/1300000009.
 8. Chandrasekhar V, Andrews J, Muharemovic T, Shen Z, Gatherer A. Power control in two-tier femtocell networks. *IEEE Transactions on Wireless Communications* Aug 2009; **8**(8):4316–4328, doi:10.1109/TWC.2009.081386.
 9. Qian L, Li X, Attia J, Gajic Z. Power control for cognitive radio ad hoc networks. *15th IEEE Workshop on Local Metropolitan Area Networks, 2007 (LANMAN'07)*, Princeton, NJ, USA, 2007; 7–12, doi:10.1109/LANMAN.2007.4295967.
 10. Sorooshyari S, Tan CW, Chiang M. Power control for cognitive radio networks: Axioms, algorithms, and analysis. *IEEE/ACM Transactions on Networking*, Jun 2012; **20**(3):878–891, doi:10.1109/TNET.2011.2169986.
 11. Grandhi S, Zander J. Constrained power control in cellular radio systems. *1994 IEEE 44th Vehicular Technology Conference*, Stockholm, Sweden, 1994; 824–828 vol.2, doi:10.1109/VETEC.1994.345205.
 12. Grandhi SA, Zander J, Yates R. Constrained power control. *Wireless Personal Communications* 1994; **1**:257–270.
 13. Yates R. A framework for uplink power control in cellular radio systems. *IEEE Journal on Selected Areas in Communications* Sep 1995; **13**(7):1341–1347, doi:10.1109/49.414651.
 14. Hanly S. An algorithm for combined cell-site selection and power control to maximize cellular spread spectrum capacity. *IEEE Journal on Selected Areas in Communications* Sep 1995; **13**(7):1332–1340, doi:10.1109/49.414650.
 15. Ogilvy CS. *Excursions in Geometry*. Dover Publications, 1990.
 16. Srinivasa S, Haenggi M. Distance Distributions in Finite Uniformly Random Networks: Theory and Applications. *IEEE Transactions on Vehicular Technology* Feb 2010; **59**(2):940–949.

17. Haenggi M. *Stochastic Geometry for Wireless Networks*. Cambridge University Press, 2012.
18. Tong Z, Haenggi M. Transport Density vs. Channel Access Time in Wireless Networks: Power Control and Efficient MAC Design. *2012 Allerton Conference on Communication, Control and Computing*, Monticello, IL, 2012.
19. Das S, Viswanathan H. A comparison of reverse link access schemes for next-generation cellular systems. *IEEE Journal on Selected Areas in Communications* 2006; **24**(3):684–692, doi:10.1109/JSAC.2005.862419.
20. Tong Z, Haenggi M. Optimizing Spatial Reuse by Dynamic Power Control. *IEEE International Conference on Communications (ICC'12)*, Ottawa, Canada, 2012.
21. Zhao Q, Sadler B. A survey of dynamic spectrum access. *IEEE Signal Processing Magazine* May 2007; **24**(3):79–89, doi:10.1109/MSP.2007.361604.
22. Lee CH, Haenggi M. Interference and outage in Poisson cognitive networks. *IEEE Transactions on Wireless Communications* Apr 2012; **11**(4):1392–1401, doi:10.1109/TWC.2012.021512.110131.
23. Chandrasekhar V, Andrews J, Gatherer A. Femtocell networks: a survey. *IEEE Communications Magazine* Sep 2008; **46**(9):59–67, doi:10.1109/MCOM.2008.4623708.
24. Khandekar A, Bhushan N, Tingfang J, Vanghi V. LTE-Advanced: Heterogeneous networks. *2010 European Wireless Conference (EW)*, 2010; 978–982, doi:10.1109/EW.2010.5483516.
25. Mathai AM. *An introduction to geometrical probability: distributional aspects with applications*. Gordon and Breach Science Publishers, 1999.